sEMG Time-Frequency Features For Hand Movements Classification

Somar Karheily, Ali Moukadem, Jean-Baptiste Courbot, Djaffar Ould Abdeslam

sEMG Time-Frequency Features For Hand Movements Classification

Somar Karheily[a,*], Ali Moukadem[a], Jean-Baptiste Courbot[a], Djaffar Ould Abdeslam[a]

[a]*IRIMAS UR 7499, Université de Haute-Alsace, Mulhouse, France*

Abstract

Surface Electro-MyoGraphic (sEMG) signals acquired on the forearm can provide information on the hand movement, which can help control a prosthetic implant for disabled people. To do so, the sEMG signals must be accurately classified despite the signals' non-stationnarity, noise from sensors, involved muscles, and patient's peculiarities. This study deals with the classification of hand movement using sEMG signals, and our main goal is to compare several feature extraction methods. We focus especially on the use of time-frequency domain for feature extraction and on several linear and non-linear methods for the dimension reduction. Methods as the Discrete Orthonormal Stockwell Transform (DOST) and Multidimensional Scaling (MDS) are applied for the first time on sEMG signals, and an extensive comparison study is performed on the combinations of the proposed methods. Classical classifiers are then used on a public dataset in order to evaluate the applied methods. Both short-time Fourier transform and Stockwell transform performed well, with respectively 90% and 91% accuracy, while promising results are obtained with DOST and MDS with classification rate 87% and significant improvement in feature extraction computation time.

Keywords: sEMG classification, Time-frequency domain, Hand gesture, non-linear dimension reduction

1. Introduction

The loss of a limb produces a permanent disability which causes a significant disruption to amputee's life. This disability has an impact of person mobility, self-care, self-image, community and leisure involvement. According to the National Limb Loss Resource Center [1], there are nearly 2 million people living with limb loss in the United States alone, with approximately 185 000 amputations occur each year, 70% of which being due to trauma involving the upper limbs.

The use of prosthetic implant can replace some of the functionality loss. These prosthetics can be controlled by users in different ways as sound, movement, electrical activity, etc. The most effective and natural way for controlling the prosthetic implant is by using the electrical activity of the muscles which is called ElectroMyoGraphy signals (EMG) and especially surface EMG (sEMG) which has the advantage of being non-invasive. However, some studies [2] observed that despite of the intensive research in prosthetic hand control over the last 60 years, there is still no system that is commercially available which satisfies all the needs of the users, and many users stop using their prosthetic after several months. In order to improve the usability of the prosthetics, more enhancement should be done in the accuracy of the patient's movement identification.

However, movements of the fingers, hand grip, or any other hand gesture, result from combinations of multiple muscles contractions in the forearm. Hence the resulting sEMG signal will contain a significant similarities which make distinguishing and classification of these sEMG a difficult challenge [3]. This is even more challenging when the person has been amputated at the forearm, because the signal level in the residual muscles is low [4]. In addition to that, the sEMG signals are non-stationary and noisy [5] which makes processing of these signals a non-trivial task.

In this paper, we aim to use sEMG to identify hand movements patterns based on time-frequency features. We use the sEMG signals from Ninapro Project [6], and time-frequency domain for features extraction which are natural candidates for non-stationary signals. Then we decrease the dimension of the extracted features by applying different dimension reduction methods (linear and non-linear), and we evaluate the improvement of the methods using different classifiers.

The main contributions of this paper can be summarized as follows:

- A detailed comparative study is carried out for feature extraction from time-frequency domain and at the level of dimension reduction methods.
- For the first time, the Discrete Orthonormal Stockwell Transform (DOST) is applied to extract features from sEMG signals, and we found that it yields competitive results while significantly reducing the computational burden.
- We also introduce the use of Multidimensional Scaling (MDS) as a non linear dimension reduction method which gave promising results.
- The proposed methods are thoroughly evaluated on a public dataset [6] and compared with state-of-the-art results.

*Corresponding author: somar.karheily@uha.fr

This paper is organized as follows: we give an introduction about sEMG signals (1.1) and related work on using these signals to identify hand movement (1.2), then we explain briefly the theoretical part of the methods we used in feature extraction (2.1) and dimension reduction methods (2.2). In the numerical experiment section (3) we explain in details the used data and the applied methods in the experiments. The results we get from each method are shown with discussion in (3.5). Finally, the conclusion of our study is given in section (4).

1.1. Electromyography Signals

EMG signals refer to the collected electric signal from muscles, which is controlled by the nervous system and produced during muscle contraction. An EMG signal is indeed the electrical activity of a muscle's motor units, which consist of two types: surface sEMG, and intramuscular EMG [7]. For prosthetic control, sEMG is preferred as it is non-invasive and more natural with no need for surgical process. Recording sEMG is performed by placing several electrodes on the skin, and different studies were performed to obtain better results in this area [8]. Over the past decades, different electrode placement strategies have been investigated. Some researchers study the use of multi-channel electrode arrays or high-density EMG strategy, while others explore the precise anatomical positioning approach [9].

When a sEMG signal is being recorded from a muscle, various types of noise will contaminate it, namely: inherent noise in the electrode, movement artifact, electromagnetic noise, cross talk, internal noise, inherent instability of the signal, and electrocardiographic artifact [5]. Therefore, analyzing and classifying EMG signals is very challenging because of the complicated patterns of EMG which is influenced by the anatomical and physiological properties of muscles [10]. These signals are a non-stationary stochastic process, and their amplitude, variance, energy, and frequency vary depending on contraction level. Typically, the amplitude ranges from 50 μV to 10 mV and frequency spectrum lies between 20 Hz and 500 Hz [11].

1.2. Related Work

1.2.1. Feature Extraction

In pattern-recognition-based control, the feature extraction and classification are crucial steps. Feature extraction involves transforming raw sEMG data into a feature vector that is used to represent a given movement. Several features extractions methods were studied in this area which can be divided into three major domains: time domain features, frequency domain features, and time-frequency domain features.

Time Domain (TD) Features. TD features are the most commonly used in sEMG signal classification [12]. Their major advantage is that they are fast to compute because no complex transformation is needed. However, because TD features are based on signal amplitude, they are relatively sensitive to noise and artifacts [13]. The most common combinations are found in Hudgin's feature vector [14], which consists of the mean absolute value, the waveform length, zero crossing, and signal slope changes. Hudgin's feature vector yields a relatively high classification accuracy, stability against changes in segment length, low discrepancy over several sessions, and computational simplicity [14][15].

In [16], Hudgin's feature vector was used and fed to a Support Vector Machine (SVM) classifier (6 classes and 4 channels) and the resulting accuracy was 96%. Note that in this case, the high classification accuracy must be tempered by the relatively low number of classes.

In a different study [17], features of sixth-order autoregressive model was added to Hudgin's feature vector, with a Linear Discriminant Analysis (LDA) as a classifier. In this study sEMG signals were recorded on 15 channels, the results of using these features were varied based on the number of classes (movements), where it was 81.0% for 29 classes, and 88.8% for 17 classes, up to 97% for 9 classes.

Another study [18] used high-density sEMG signals, by recording sEMG signals of the forearm using an array of 192 electrodes. Root mean square values were used as a feature for each signal, and an average of 95% of classification rate for 9 classes is reached with a SVM classifier.

Despite the fact that TD features are simple to compute and could perform well for prosthetic with a few degrees of freedom (i.e. less classes), the nature of sEMG signals and its non-stationary characteristic make the TD features limited to preserve intrinsic features of the sEMG signals.

Frequency Domain (FD) Features. FD features can be used to estimate muscle fatigue, force production and changes in muscle activation patterns [13]. Using FD features alone in movement pattern recognition has not given good results compared to TD features which outperformed the frequency features and were more stable [13].

The studies addressing feature extractions show that using the TD features gives better results than using FD features. In [12] frequency domain features alone were tested, which are mean frequency, Median frequency, 1st, 2nd and 3rd spectral moments and frequency ratio. In this study, the FD features classification accuracy was between 75-85% where most of the used TD features accuracy was more than 85% for six upper limb movements applied on the same dataset.

However, combining FD features with successful TD features may yield more robust classification than TD features. In two studies [19][20], appending the mean and median frequency to TD features increased the robustness of the classification. Different sets of features in noisy environment were tested in study [20] and it was approved that by appending these two TF features, the error rate decreased from 20% to 5-10% for six upper limb motions.

Time-Frequency Domain (TFD) Features. TFD features contains the combination of temporal and frequency information. These features characterize the signal in a time-frequency plane which allows an accurate description of the variability of frequency over time, providing plentiful non-stationary information about the sEMG signals.

Recent studies have shown that time-frequency analysis methods can extract relevant information about sEMG signals [21][22], but on the other hand they yield a high-

dimensional feature vector. Hence using all the features would be numerically intractable and weakly relevant to the classification. Therefore it is mandatory to perform a dimension reduction on these features. Several time-frequency methods were used in the state of the art.

Short Time Fourier Transform (STFT) [23] is a well-known time-frequency method which performs a mono-resolution analysis by applying a fixed-size window on the signal. STFT was successfully used to extract intrinsic features of the movement identification, and led to high classification rate in case of large training data when followed by linear or non-linear dimension reduction methods [22] where the average accuracy was of 94.8% for six hand motions with 90% training set size. However, it may be limited in term of time-frequency resolution for some non-stationary signals, where we need to adapt the resolution of the analyzing window over the frequency of the signal.

The Wavelet Transform (WT) overcomes the shortcomings of frequency-invariant window in the STFT. The WT adapts to the change in frequency in the signal by scaling the mother wavelet. When the frequency in the signal increases, the WT increases the resolution by narrowing the used wavelet. In [15][24] the Continuous WT (CWT) was used and proved to outperform TD features when applied on different datasets, while in [25] Discrete WT (DWT) was proven to provide sufficient information about the original signal, with a significant reduction in the computation time compared to STFT.

The Stockwell Transform (ST) is a time-frequency analysis method, and is a hybrid version between the STFT and the CWT. It uses a multi-resolution Gaussian window by varying its standard deviation over the analyzed frequencies [26]. Unlike the wavelet transform, the ST preserves the phase information of the signal in the same way as the Fourier transform. A recent study [27] shows that ST features overcomes wavelet packet transform features for sEMG classification, where three levels of wavelet decomposition and symmlet mother wavelet of order five were adopted in this research. The ST achieved 98.12% of average accuracy for six hand motions while wavelet packet transform achieved 97.61% [27].

1.2.2. Dimension Reduction and Classification

The dimension reduction becomes an essential part when dealing with TF features because of their high-dimensional space. One of the most used dimension reduction technique is the Principal Component Analysis (PCA) [28] as a linear dimension reduction method. In [29] PCA was applied to reduce dimension of the wavelet packet transform features, and the final classification accuracy result was 96% accuracy on 9 different classes.

Dimension reduction has been notably generalized since the introduction of non-linear techniques, which do not require the low-dimensional space to be Euclidean. A study [22] compared PCA and Diffusion Maps (DM), when applied on STFT features. This study concluded that DM outperforms PCA when less training data is available. This point is important, as training effort is one of the challenges that faces prostheses development. Another study [30] shows how the features' dimension reduction process can improve the classification of sEMG in armband acquisition approach. This study found that, with respect to several other dimension reduction techniques, the best results in this study were obtained by using the Large Margin Nearest Neighbor (LMNN) and a SVM classifier with 94% accuracy for six wrist movements.

Regarding the classification step, several methods were used to classify sEMG signals as k-Nearest Neighbors (k-NN) [31], LDA [32], SVM [33], Neural networks (NN) [34]. A study [35] made a comparison between k-NN and SVM when applied on the TF features of sEMG signals. Both methods performed well on these kind of features with better accuracy score for k-NN. For 15 fingers' motions, k-NN with PCA had average accuracy of 93.76% while SVM with PCA had 88.88%.

2. Methods

We saw that TF features and DR play an essential part in modern sEMG classification and they give promising results in the literature. However, there is no comprehensive work on this topic. In this paper, we will test a new time-frequency method (DOST) and compare it to other classical TF methods, in combination with several DR methods, in order to classify sEMG signals.

Data used in this work [6] is recorded by surface electrodes placed on the arm of the subject, and each movement is repeated several times. The data is saved in a matrix $E \in \mathbb{R}^{n\times m}$, where n is the total number of recorded samples on a channel for all movements together, and m is number of channels (electrodes). For a single observation e in that matrix, we have number p of samples on each channel, where p is based on the chosen segment length, so that $e \in \mathbb{R}^{p\times m}$. In this section, we will detail the methods used in our study at each stage of features' extraction, dimension reduction and classification.

2.1. TF Feature extraction

We apply three different TF transforms (STFT, ST, and DOST) in order to evaluate the efficiency of these features based on classification accuracy. We use STFT as it is used in literature [23] and it yields promising results, while ST is chosen because it extends STFT by performing multi-resolution analysis. According to our knowledge, for the first time the DOST is applied in this paper on the sEMG signals, and it has the advantage of its efficient computational complexity.

2.1.1. Short Time Fourier Transform

STFT overcomes the disadvantages of the frequency domain alone by considering frequency variations over the time, which is necessary for sEMG as it is non-stationary signal. It is applied using a sliding window in which we consider the signal as stationary. Therefore, the Fourier transform can be applied in order to obtain the local spectrum [36] as follows:

$$\mathrm{STFT}(\tau, f) = \int_{-\infty}^{+\infty} s(t)g(t-\tau)e^{-i2\pi ft}dt; \qquad (1)$$

where $s(t) \in L^2(\mathbb{R})$ is the original signal, $t, \tau \in \mathbb{R}$ refers to time, $f \in \mathbb{R}^*$ the frequency, and $g(t) \in L^2(\mathbb{R})$ is the applied window function. We chose a Gaussian window for STFT transform, in order to compare with ST. In addition, the Gaussian window minimize the Heisenberg-Gabor relation which describes the compromise between the time and frequency resolution. Using the standard deviation σ, $g(t)$ is written:

$$g(t) = \frac{1}{\sigma\sqrt{2\pi}} e^{\frac{-t^2}{2\sigma^2}}. \quad (2)$$

2.1.2. Stockwell Transform

The Stockwell transform is an hybrid version between the STFT and CWT. It uses a multi-resolution Gaussian window by varying its standard deviation over the analyzed frequencies [26]. The ST, as defined originally by Stockwell et al. [37], can be derived from Eq.(1) by replacing σ in (2) by $1/|f|$. Then the window function can be expressed as follows:

$$g(t) = \frac{|f|}{\sqrt{2\pi}} e^{\frac{-t^2 f^2}{2}}. \quad (3)$$

Then the ST is defined as [37]:

$$ST(\tau, f) = \int_{-\infty}^{+\infty} s(t) \frac{|f|}{\sqrt{2\pi}} e^{\frac{-(t-\tau)^2 f^2}{2}} e^{-i2\pi f t} dt. \quad (4)$$

Then, the discrete ST is defined as follows: let $s[kT] \in L^2(\mathbb{R})$ with $k = 0, 1, \ldots, N-1$ denote the discrete time series corresponding to $s(t)$ with a time sampling interval of T. The discrete Fourier transform (DFT) of $s[kT]$ is obtained as:

$$S[\frac{n}{NT}] = \frac{1}{N} \sum_{k=0}^{N-1} s[kT] e^{\frac{-i2\pi nk}{N}}; \quad (5)$$

where $n = 0, 1, \ldots, N-1$.

By setting $f = n/NT$ and $\tau = jT$ in Eq(4), and by writing the ST as a convolution product, we can get a direct link between ST and the Fourier transform of the analyzed signal S and the Fourier transform of the Gaussian window $e^{\frac{-2\pi^2 m^2 \alpha^2}{n^2}}$ as follows :

$$S[jT, \frac{n}{NT}] = \sum_{m=0}^{N-1} H[\frac{m+n}{NT}] e^{\frac{-2\pi^2 m^2 \alpha^2}{n^2}} e^{\frac{i2\pi mj}{N}}; \quad (6)$$

which is optimized for implementation with respect to Eq. (5), because of its relation to FFT.

2.1.3. Discrete Orthonormal Stockwell Transform (DOST)

For a signal of length N, there are N^2 Stockwell coefficients, and their computation has a $O(N)$ time complexity. Hence, computing all N^2 coefficients of the ST has a computational complexity of $O(N^3)$, so the ST gets very expensive for high-dimension space.

The DOST prunes the redundancy in within the ST. Indeed, since lower frequencies have longer periods, they can cope with lower sampling rates. Hence, the DOST down-samples the low frequencies. Conversely, high frequencies have a higher sampling rates.

The DOST takes advantage of this sample spacing paradigm, and distributes its coefficients accordingly. It does so by constructing a set of N orthogonal unit-length basis vectors, each of them targeting a particular region in the time-frequency domain [38][39]. Thus the DOST representation can be defined as the inner products between a time series $s[kT]$ and the orthonormal basis functions defined as function of $[kT]$, with the parameters ν (a frequency variable locating the center of a frequency band), β (defining the frequency resolution), and τ (for time localization):

$$Sh[kT] = S(\tau T, \frac{\nu}{NT}) = \sum_{k=0}^{N-1} h[kT] S_{[\nu,\beta,\tau]}[kT]; \quad (7)$$

where:

$$S_{[\nu,\beta,\tau]}[kT] = \frac{ie^{-i\pi\tau}}{\sqrt{\beta}} \frac{e^{-i2\pi(\frac{k}{N}-\frac{\tau}{\beta})(\nu-\frac{\beta}{2}-\frac{1}{2})} - e^{-i2\pi(\frac{k}{N}-\frac{\tau}{\beta})(\nu+\frac{\beta}{2}-\frac{1}{2})}}{2\sin[\pi(\frac{k}{N}-\frac{\tau}{\beta})]}. \quad (8)$$

The following rules needs be applied to the sampling of the time–frequency space to ensure orthogonality [39]

- τ = 0, 1,...,β-1.
- ν and β must be selected such that each Fourier frequency sample is used once and only once.

2.2. Dimension Reduction

The final output of the features extraction is $F \in \mathbb{R}^{N\times k}$ where N is the number of observations and k is the number of TF features for each observation. F contains all observations' features, and it belongs to a high dimensional space (typically, $k \approx 3 \times 10^6$): this makes dimension reduction a mandatory step. In this paper, we apply both linear and nonlinear methods in order to study the best approach that should be used in this area.

Each dimension reduction method takes the features' matrix $F \in \mathbb{R}^{N\times k}$ as an input and yields the reduced features' matrix $Y \in \mathbb{R}^{N\times d}$ where $d \ll k$.

A baseline for dimension reduction consists in Principal Component Analysis (PCA), which is one of the most popular linear dimension reduction [28].

2.2.1. Multidimensional Scaling (MDS)

MDS [40] methods aim to reduces the dimension of the data by using only the dissimilarities measures between observations rather than using the data points. The idea is to find a lower-dimensional representation of the data that preserves the pairwise distances as well as possible [41].

Nonclassical multidimensional scaling creates a configuration of points whose inter-point distances approximate the given dissimilarities. In our study we used non-metric scaling which is designed to relax this condition. Instead of trying to approximate the dissimilarities themselves, non-metric scaling approximates a nonlinear, but monotonic, transformation of these dissimilarities. Because of the monotonicity, larger or smaller distances on a plot of the output will correspond to larger or

smaller dissimilarities, respectively. Nonmetric MDS creates a configuration of points whose inter-point distances approximate a monotonic transformation of the original dissimilarities [40][42].

The steps of MDS are the following [43]:

- From the features matrix F, we calculate the inter-point distances matrix $D \in \mathbb{R}^{N\times N}$, the elements of D denoted d_{ij} are, $\forall i, j \in \{1, \ldots, N\}$:

$$d_{ij} = \|F_i - F_j\|_2 \text{ where } F_i, F_j \in F \tag{9}$$

- From D, we form the matrix A so that $\forall i, j \in \{1, \ldots, N\}$:

$$a_{ij} = [-\frac{1}{2} d_{ij}^2] \tag{10}$$

- Then we apply double centering:

$$B = HAH \tag{11}$$

  where H is the centering matrix: $H = I - \frac{1}{N} 1_N 1_N^T$ with 1_N a vector of ones.

- Next, we calculate the spectral decomposition of B

$$B = \mathcal{V}\Lambda\mathcal{V}^T \tag{12}$$

  where Λ is the diagonal matrix formed from the eigenvalues of B, and $\mathcal{V}$ is the matrix of corresponding eigenvectors. To get the embedded features in the $p-$dimensional space, we take the first p eigenvalues as Λ_p and first p eigenvectors as $\mathcal{V}_p$

- The new embedded features matrix Y is:

$$Y = \mathcal{V}_p \Lambda_p^{\frac{1}{2}} \tag{13}$$

The new dimension $p \ll k$ should be chosen so that features still preserve intrinsic characteristics of the observation, while removing weakly-relevant or redundant information.

2.2.2. Isomap

Isomap [44] stands for isometric mapping, and assumes that the data in the high-dimensional space lies on some manifold. Isomap is a non-linear dimension reduction method which aims at preserving the geodesic distances in the lower dimension. It constructs a graph that approximates the geodesic distances of the points in the manifold, then it considers this graph as an approximation of the manifold.

In our case, the manifold is the feature matrix $F \in \mathbb{R}^{N\times k}$, containing the TF features. The first step in Isomap is to compute the inter-point Euclidean distances matrix $D \in \mathbb{R}^{N\times N}$ (Eq. (9)) between each element of F. Then, we define the initial distance matrix $P \in \mathbb{R}_+^{N\times N}$ such that each element p_{ij} is, $\forall i, j \in \{1, \ldots, N\}$:

$$p_{ij} = \begin{cases} p_{ij}, & \text{if } F_j \text{ belongs to the } u \text{ nearest neighbors of } F_i \\ \infty, & \text{otherwise} \end{cases} \tag{14}$$

P serves as an adjacency matrix in order to build a graph $\mathcal{G}$ which approximates the manifold supporting F.

In its second step, Isomap estimates the geodesic distances between all pairs of points by computing the shortest path on $\mathcal{G}$ using Dijkstra's algorithm. This yields a geodesic distance matrix $D_{\mathcal{G}} \in {\mathbb{R}_+}^{N\times N}$, which represents the new kernel of the initial manifold. Finally, we calculate the spectral decomposition of $D_{\mathcal{G}}$ and the new embedded features matrix Y in the same way as in Eqs. (12,13).

2.2.3. Diffusion Maps (DM)

DM aims to reduce the dimension of a high-dimensional dataset while preserving the local and global geometry [22]. The kernel in DM method (Gaussian kernel) defines the connectivity of each point with its neighbourhood, where this connectivity measure drops quickly to zero for weak connected neighbours. Using a Gaussian kernel has special characteristics:

- Values in the kernel decrease with distance and goes to zero for far points which more likely belong to different cluster or kind.
- It is bounded between zero and one, so it is less sensitive to abnormal observations.

The first step in this method is to calculate the positive weight matrix $W \in \mathbb{R}_{+*}^{N\times N}$ such that $w_i j$ is, $\forall i, j \in \{1, \ldots, N\}$:

$$w_{ij} = e^{-\frac{\|F_i - F_j\|_2^2}{2\sigma}}. \tag{15}$$

Then, a normalized kernel matrix $A \in \mathbb{R}_{+*}^{N\times N}$ is computed, $\forall i, j \in \{1, \ldots, N\}$:

$$a_{ij} = \frac{w_{ij}}{\sum_{i=1}^{N} w_{ij} \times \sum_{j=1}^{N} w_{ij}} \tag{16}$$

After that we produce the Markov transition matrix $M \in]0, 1]^{N\times N}$ such that $\forall i, j \in \{1, \ldots, N\}$:

$$m_{ij} = \frac{a_{ij}}{\sum_{i=1}^{N} a_{ij}} \tag{17}$$

M is a normalized version of A so that it is analog to a probability of moving from F_i to F_j.

The final step is similar to previous the dimension reduction methods, as we calculate the spectral decomposition of the matrix M and the embedded features matrix Y, see Eq(12,13).

2.3. Classification

Several classification algorithms have been used in sEMG signals classification with different combinations of features and classifiers [10][13][45]. In order to evaluate the methods we use in features extraction and dimension reduction, we choose three of the most used classifiers in the literature:

- k-nearest neighbors (k-NN) algorithm, which classifies data point based on the points that are nearest to it [31]

- Linear discriminant analysis (LDA), which is based on the probability that a point belongs to each class. The point is classified as the class with the highest probability which is estimated using Bayes Theorem [32].

- Support vector machine (SVM), which tries to project the feature space into a larger dimension space, by using a kernel function, in order to separate the transformed data linearly. SVM doesn't support multi-class classification natively. It supports binary classification and separating data points into two classes. Multi-class SVMs (MCSVM) are implemented by combining several binary SVMs [33][46].

In the following, we will compare the results of these three classifiers in combination with different TF and DR methods.

2.4. Main Algorithm

Starting from raw sEMG data, the main steps of the proposed algorithms in our paper are the following:

- Data normalization: we first normalize the data so we get standard deviation 1, and mean values 0 on each channel. The normalized data is $S \in \mathbb{R}^{n\times m}$, where m is the number of channels and n is the total number of signal's samples on each channel, will be used in features extraction.

- Time-frequency features extraction: time-frequency transform is applied on the normalized signals of each channel. Then for each observation, we combine the result into a single vector of length k. The resulting features matrix for all observation is $F \in \mathbb{R}^{N\times k}$ where N is number of observations (data points).

- Dimension reduction of the features space: we apply dimension reduction methods to transform the feature matrix $F \in \mathbb{R}^{N\times k}$ into a more compact $Y \in \mathbb{R}^{N\times d}$ where $d \ll k$.

This algorithm is summarized in figure 1.

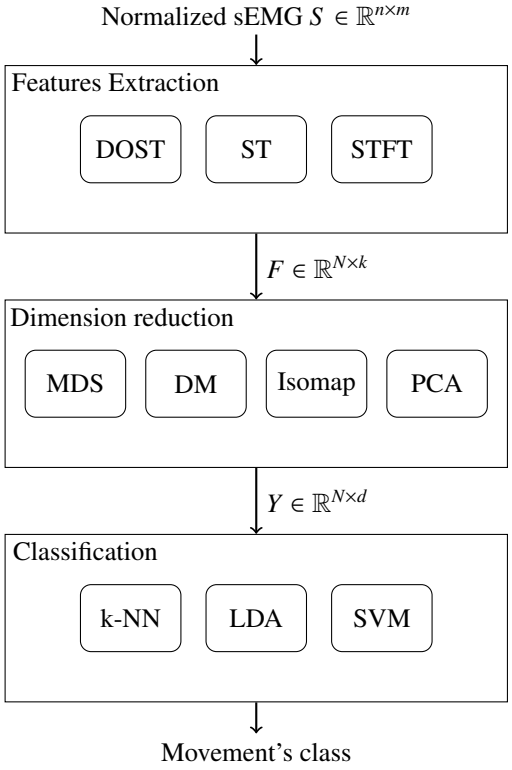

Figure 1: The main algorithm of the paper. It shows the data flow starting from the normalized sEMG signals; and how the data processed until the classification. In this paper, we compare the different combination possibilities for each step.

3. Numerical experiments

3.1. Data

In order to evaluate the chosen methods we used the database provided by the Ninapro Project [6]. The advantages of this database is that it contains recorded data for wide range of movements and for many subjects, which provides good resource for training and testing. All this data is recorded in a unified format which is useful when comparing our applied methods. We chose exercise 1 from database 2, which contains 17 different basic movements of fingers and wrist. The sEMG signals are provided together with their hand gestures. Each movement in the exercise is repeated 6 times, where each subject was asked to repeat movement and hold position for 5 second, followed by 3 second of rest. The muscular activity is sampled at a rate of 2 kHz by $m = 12$ electrodes placed on subject's arm. The recorded sEMG data is saved into the matrix $E \in \mathbb{R}^{n\times m}$ where n is the number of recorded samples on one channel. Figure 2 shows the list of these basic hand moves.

3.2. Feature extraction

3.2.1. Feature's sliding window

Due to real-time constraints, an adjacent segment length plus the processing time of generating classified control commands should be equal or less than 300 ms [47], while the segment should be long enough to have sufficient features for classification. Therefore a tradeoff in response time and accuracy should be considered when selecting the window length. In our experiments we chose the window length equal to 250 ms with 125 ms overlapping as it is used in studies with similar constraints [48][49][50]. The sampling frequency is 2 kHz, for each observation we get 12 windows (i.e. 12 electrodes) with 250 ms length. In figure 3 we can see an example of observation windows on one of the channels.

3.2.2. TF features

After segment extraction we get 12 windows for each single observation. We apply the TF method on each of them, and then we yield the resulting matrix into a vector. Finally we combine all these 12 vectors into one vector F_i which represents the TF features of this observation $F_i \in \mathbb{R}^k$ where k is the number of TF features of a single observation. For each observation in the dataset, we extract the features' vector in the same way, then we save it into the feature matrix $F \in \mathbb{R}^{N\times k}$ where N is the number of observations.

We use a sampling frequency of 2 kHz, with a frequency range between 1 and 200 Hz, as the usable energy of sEMG

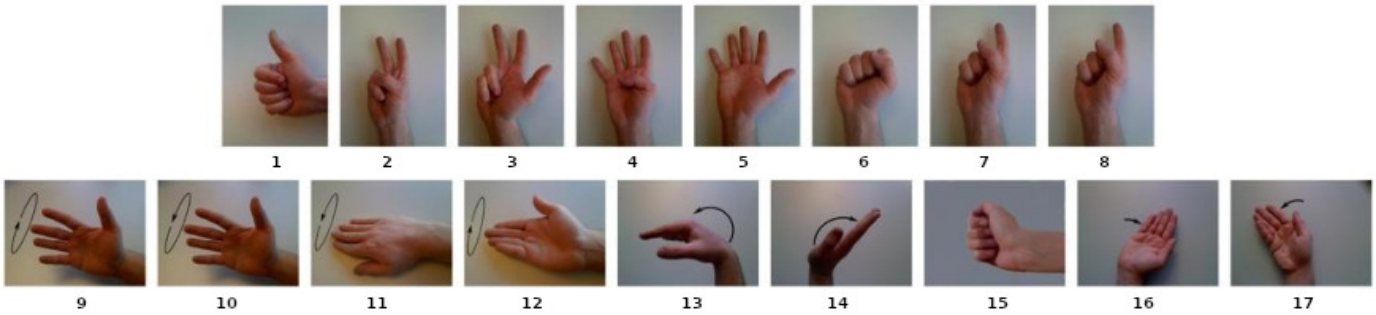

Figure 2: Visual depiction of the 17 hand gestures considered in our study, based on the NinaPro database [6]

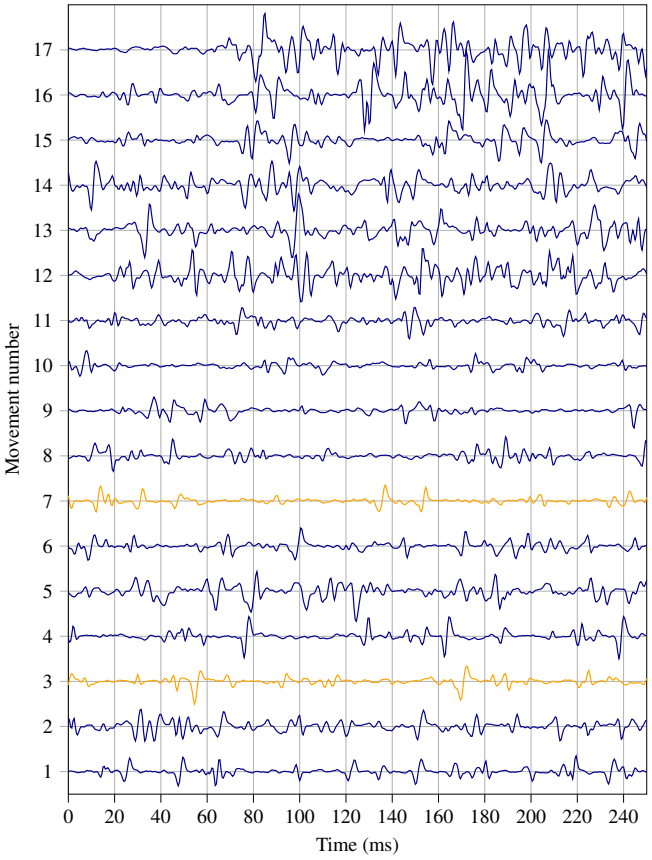

Figure 3: Example of recorded signals on channel 1 for the 17 movements (see 2). TF of the highlighted movement are shown in Fig.4.

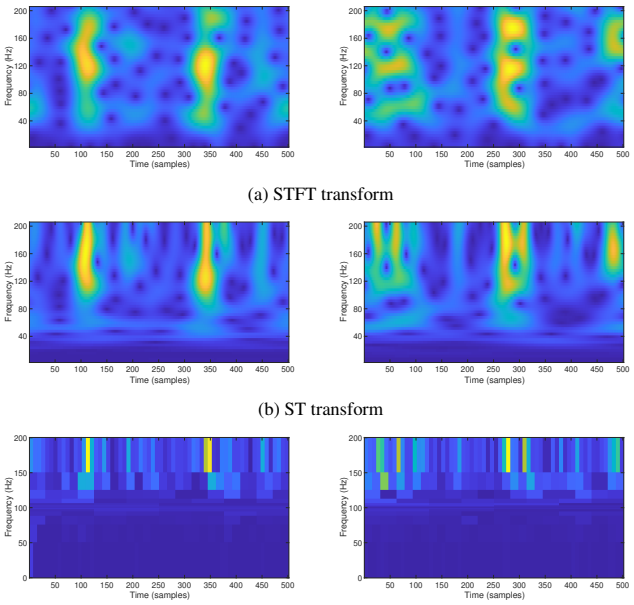

(a) STFT transform

(b) ST transform

(c) DOST transform, rearranged to give a TF representation.

Figure 4: TF transforms examples: to the left is movement 3 - channel 1, to the right is movement 7 - channel 1. Movements are shown in figure 2

signal is dominant in this range.
Given these values, the number of TF features k on a single observation is $k \simeq 3.10^5$ for STFT and ST, while $k \simeq 6.10^3$ for the DOST. For the STFT we choose empirically the value $\sigma = 0.03$ (see Eq. (2)) since it gives a good compromise between time and frequency resolutions. For the ST, we keep the original version where $\sigma = 1/|f|$. Similarly, for the DOST, the original version proposed by [39] is applied in this paper.
Figure 4 depicts an instance of STFT, ST, and DOST transforms applied on the same sample.

Note that in practice, we observe a significant drop in computation time when using the DOST, which takes around 8% of the required time for STFT or ST (table 1). In addition the DOST output lies in a lower-dimensional space.

Method	Time(ms)
STFT	1.75
ST	1.60
DOST	0.13

Table 1: TF feature computation time on window of one channel, calculated as an average over all 39360 samples windows in the dataset

3.3. Dimension reduction

For all methods applied in dimension reduction, the input is the features matrix $F \in \mathbb{R}^{N\times k}$, with k depending on the method used in previous step. The number of features which we want to reduce the space into is important as selecting more features will lead to over fitting in the classification, and selecting less than needed will lose valuable data in the features and in both cases the classification accuracy will be worse.

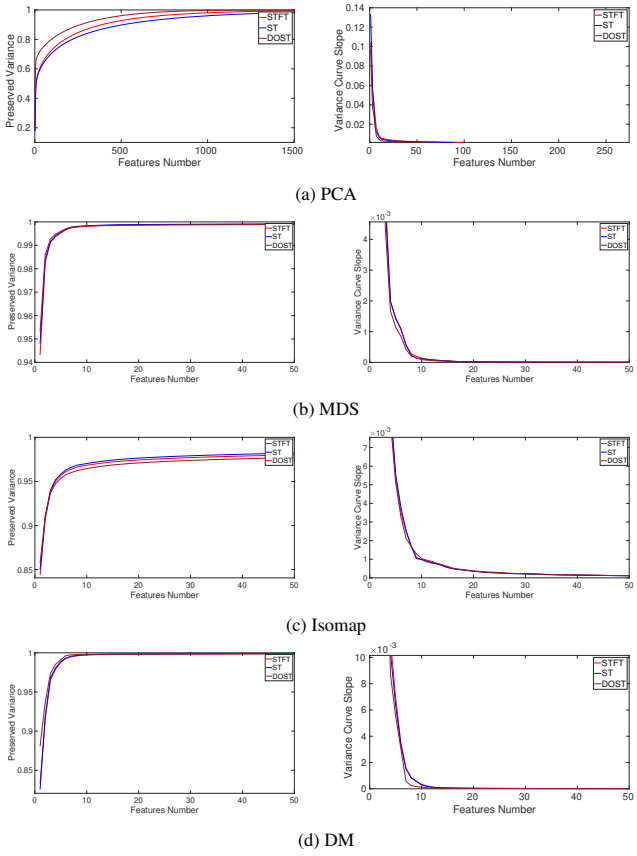

(a) PCA

(b) MDS

(c) Isomap

(d) DM

Figure 5: Preserved variance by number of features in the embedded space

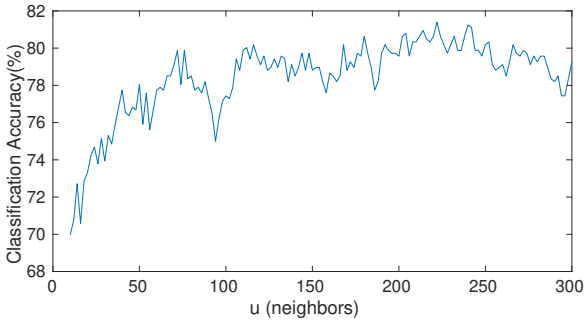

Figure 6: Isomap - Classification accuracy by number of neighbours in Isomap algorithm

3.4. *Classification*

For the k-NN classifier, we choose value of 3 nearest neighbors, as it gave better results on our data, and for SVM, we choose the Gaussian kernel function and combine several one-versus-one of multiple binary SVMs. Each combination is evaluated based on K-fold Cross-Validation with value $K = 5$.

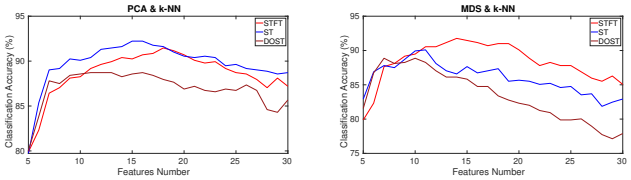

Figure 7: Classification accuracy by features number

For PCA, the dimension of the new embedded space is decided based on the preserved variance in Figure 5a we see the preserved variance by features number and the slop which presents the changing rate of the preserved variance. We test different values of embedded features number in a range where preserved variance stop increasing rapidly. Finally, we choose the value of d with the best accuracy (figure 7).

For the non-linear methods, the original space of the features matrix is replaced by a kernel of paired similarity/dissimilarity, and then PCA is applied on this kernel. Therefore, we use the variance of the new kernel as a factor for choosing the new dimensions. In each case we approved our concept by testing values that belong to interval where the ratio between preserved variance and features number is increasing significantly by features number increment. Figures 5b, 5c, 5d show relation between the preserved variance and the number of the features in the embedded space for kernels of MDS, Isomap, DM respectively. and figure 7 shows classification accuracy by number of embedded features for non-linear methods.

Isomap requires the setting of an additional parameter, namely the value u (number of neighbours to be considered when building the graph) which gives best results in classification, so we run our tests for all u values $[10, 300]$ as values more than that will leads to multiple clusters being considered as neighbours in Isomap algorithm. We chose $u = 220$ based on this test as shown in figure 6.

3.5. *Results and Discussion*

A summary of the classification accuracy obtained by varying TF, DR and classification methods, averaged over five different subjects, is given in table 2. As we see in the table, both STFT and ST are approximately giving the same performance with slight advantage for the ST features. The best combination we got was by using ST features and PCA for dimension reduction and k-NN as classifier which yields a 90.96% accuracy.

Comparing TF methods. As we see from the results, ST performance is slightly better than STFT due to its multi-resolution nature, also it adapts better to the variation of the frequency content of the sEMG signal comparing to the STFT, which can enhance the quality of the extracted features. DOST gives less accuracy with no noticeable difference from both STFT and ST. DOST preserves information in time-frequency domain in a non-redundant approach (due to the used orthogonal basis) and it has a $O(N)$ time complexity (to be compared to $O(N^3)$ for other TF methods) that's explains why in our practical experiments the DOST was more than 10 times faster on our testing platform[1] (see table 1). This criteria is an important advantage for the DOST as it makes it possible for real prosthetic application when processing time is very critical factor and the processing power is limited. However, rigorously speaking, the

[1] Intel(R) Core(TM) i7-9750H CPU @ 2.60GHz - 64 GB Ram

DOST is not exactly the orthonormal version of the ST. As shown in [51], the classical DOST version applies the equivalent of a boxcar window and not a Gaussian one as ST. This can explain the slightly decreasing performance for the classification rate for the DOST.

Comparing DR methods. For the dimension reduction methods, PCA yields better results than non-linear dimension reduction methods, then comes MDS which outperformed Isomap and DM. The proposed method MDS still performs less than PCA, but based on a study [22] which compared PCA with DM on STFT features; it was proved that non-linear dimension reduction outperforms PCA when less training data is used. Training data size is an important factor as it reflects the time and effort needed by the amputee to be able to use his prosthetic. Non-linear dimension reduction methods is based completely on the constructed kernel that describes similarity/dissimilarity between paired observations, and the fact that they perform less that PCA could be because that we need better way to measure the similarity between observations.

Comparing classification methods. k-NN classifier is giving better classification accuracy. These results is consistent with some studies which did comparison between classifiers on sEMG signals. In [35] both k-NN and SVM were applied on TF features with PCA as dimension reduction method and k-NN outperformed SVM. Another study [52] did comparision between k-NN and LDA classifiers on sEMG signals of wrist motions and they concluded that k-NN has better average recognition rate.

For the purpose of comparing combinations of TF methods with DR methods, we observed that the methods combination that leads to better accuracy using k-NN classifier is also giving better accuracy than other methods combinations using LDA and SVM, which means, changing the classifier will not promotes one combination over the other.

Other studies on the same dataset. We can compare the TF features to other TD and FD features, by comparing to other studies using TD or FD features on the same dataset and same exercises. In [53] different combinations of TD features were tested with different classifiers on the same dataset. Classification, using a k-NN classifier, yields then a 85% accuracy. Another study [54] used TD with FD features (RMS and median frequency) with paraconsistent artificial neural network classifier and achieved a 76,0±9,1% accuracy. Comparing these results to our study, we proved that TF features outperform TD and FD features, even when using the time-efficient DOST method.

TF	DR	d	Classifier	Acc. (%)	Time(s)
STFT	PCA	18	k-NN	**90.05**	167.73
			LDA	81.78	167.75
			SVM	84.48	168.75
	MDS	14	k-NN	**87.88**	91.14
			LDA	77.76	91.18
			SVM	82.84	92.10
	Isomap	14	k-NN	**79.17**	688.00
			LDA	73.50	688.40
			SVM	75.03	689.50
	DM	14	k-NN	**86.09**	95.44
			LDA	79.42	95.48
			SVM	83.17	96.98
ST	PCA	15	k-NN	**90.96**	179.52
			LDA	83.62	180.00
			SVM	85.63	181.20
	MDS	11	k-NN	**88.99**	89.54
			LDA	77.60	89.98
			SVM	82.58	100.40
	Isomap	11	k-NN	**81.10**	695.37
			LDA	73.11	695.80
			SVM	75.11	696.73
	DM	11	k-NN	**87.91**	87.92
			LDA	82.17	88.35
			SVM	84.70	89.44
DOST	PCA	11	k-NN	**88.08**	15.65
			LDA	80.40	15.69
			SVM	82.31	16.28
	MDS	10	k-NN	**87.13**	28.21
			LDA	72.68	29.03
			SVM	75.74	29.64
	Isomap	10	k-NN	**76.88**	589.33
			LDA	70.23	589.81
			SVM	72.73	590.73
	DM	10	k-NN	**85.22**	13.42
			LDA	78.14	13.77
			SVM	81.60	14.80

Table 2: The final classification results of all combinations of the used methods with their computation time. The classification rate for each combination were calculated using cross-validation method and an average of accuracy for 5 subjects. TF: time-frequency method, DR: dimension reduction method, d: the number of features in the embedded space, Acc.: the classification accuracy, Time: the overall time for feature extraction, dimension reduction and training.

4. Conclusion

We applied different kinds of TF features and proved their efficiency for sEMG classification problems over TD features. We proposed using DOST which is time-efficient with no significant drop in accuracy, and that makes it applicable in real prosthetic application. We also proposed using MDS as non-linear dimension reduction method, and the importance of non-linear methods comes from the fact that they require less training data, which is one of the problems that face the development of prosthetic. In this study we made extended review about combinations of TF features and dimension reductions method and provided these combination results applied on the same data. The best combination is achieved by using ST with PCA and k-NN where the classification accuracy is 90.96%. Taking the computation time in consideration promotes using DOST with PCA and k-NN where the classification accuracy is 88.08%.

This study should help in taking decisions about choosing the TF and dimension reduction methods, and pave the way to more advanced studies in one or more of these combinations. Future work will be about non-linear method optimizing to more

suits the used features, besides to more experiments on cross-subjects features using these methods.

References

[1] K. Ziegler-Graham, E. MacKenzie, P. Ephraim, T. Travison, R. Brookmeyer, Estimating the prevalence of limb loss in the united states: 2005 to 2050, Archives of physical medicine and rehabilitation 89 (3) 422–429. doi:10.1016/j.apmr.2007.11.005.

[2] D. Farina, N. Jiang, H. Rehbaum, A. Holobar, B. Graimann, H. Dietl, O. Aszmann, The extraction of neural information from the surface EMG for the control of upper-limb prostheses: emerging avenues and challenges, IEEE Trans Neural Syst Rehabil Eng Jul;22(4):797-809, epub 2014 Feb 11. PMID: 24760934. doi:10.1109/TNSRE.2014.2305111.

[3] M. Gazzoni, N. Celadon, D. Mastrapasqua, M. Paleari, V. Margaria, P. Ariano, Quantifying forearm muscle activity during wrist and finger movements by means of multi-channel electromyography, PLoS One 7;9(10):e109943, pMID: 25289669; PMCID: PMC4188712. doi:10.1371/journal.pone.0109943.

[4] L. Pizzolato, Tagliapietra, M. Cognolato, M. Reggiani, H. Müller, M. Atzori, Comparison of six electromyography acquisition setups on hand movement classification tasks, PLoS ONE 12 (10) (2017) e0186132. doi:10.1371/journal.pone.0186132.

[5] R. Chowdhury, M. Reaz, M. Ali, A. Bakar, K. Chellappan, T. Chang, Surface electromyography signal processing and classification techniques, Sensors (Basel 17;13(9):12431-66, pMID: 24048337; PMCID: PMC3821366. doi:10.3390/s130912431.

[6] M. Atzori, A. Gijsberts, C. Castellini, B. Caputo, A.-G. M. Hager, S. Elsig, G. Giatsidis, F. Bassetto, H. Müller, Electromyography data for non-invasive naturally-controlled robotic hand prostheses, Scientific data 1 (1) (2014) 1–13.

[7] L. J. Hargrove, K. Englehart, B. Hudgins, A comparison of surface and intramuscular myoelectric signal classification, IEEE Transactions on Biomedical Engineering 54 (5) (2007) 847–853. doi:10.1109/TBME.2006.889192.

[8] Y. Blanc, U. Dimanico, Electrode placement in surface electromyography (semg)"minimal crosstalk area"(mca), The Open Rehabilitation Journal 3 (2010) 110–126. doi:10.2174/1874943701003010110.

[9] H. Hermens, B. Freriks, The state of the art on sensors and sensor placement procedures for surface electromyography: A proposal for sensor placement procedures.

[10] N. Nazmi, M. Abdul Rahman, S. Yamamoto, S. Ahmad, H. Zamzuri, S. Mazlan, A review of classification techniques of EMG signals during isotonic and isometric contractions, Sensors (Basel 17;16(8):1304, pMID: 27548165; PMCID: PMC5017469. doi:10.3390/s16081304.

[11] N. Meselmani, M. Khrayzat, K. Chahine, M. Ghantous, M. Hajj-Hassan, Pattern recognition of EMG signals: Towards adaptive control of robotic arms, in: 2016 IEEE International Multidisciplinary Conference on Engineering Technology (IMCET), 2016, pp. 52–57. doi:10.1109/IMCET.2016.7777426.

[12] A. Phinyomark, P. Phukpattaranont, C. Limsakul, Feature reduction and selection for EMG signal classification, Expert Syst. Appl. 39 (2012) 7420–7431.

[13] M. Hakonen, H. Piitulainen, A. Visala, Current state of digital signal processing in myoelectric interfaces and related applications, Signal Processing and Control P. 334-359 1746–8094, printed). DOI: 10.1016/j.bspc.2015.02.009.

[14] B. Hudgins, P. Parker, R. N. Scott, A new strategy for multifunction myoelectric control, IEEE Transactions on Biomedical Engineering 40 (1) (1993) 82–94. doi:10.1109/10.204774.

[15] K. Englehart, B. Hudgins, A robust, real-time control scheme for multifunction myoelectric control, IEEE Transactions on Biomedical Engineering 50 (7) (2003) 848–854. doi:10.1109/TBME.2003.813539.

[16] M. Oskoei, H. Hu, Support vector machine-based classification scheme for myoelectric control applied to upper limb, IEEE Transactions on Engineering 55 (8) 1956–1965,. doi:10.1109/TBME.2008.919734.

[17] D. Tkach, A. Young, L. Smith, E. Rouse, L. Hargrove, Real-time and offline performance of pattern recognition myoelectric control using a generic electrode grid with targeted muscle reinnervation patients, IEEE Trans Neural Syst Rehabil Eng Jul;22(4):727-34, epub 2014 Feb 11. PMID: 24760931. doi:10.1109/TNSRE.2014.2302799.

[18] M. Rojas-Martínez, M. A. Mañanas, J. Alonso, High-density surface EMG maps from upper-arm and forearm muscles, Journal of NeuroEngineering and Rehabilitation 9 (2011) 85 – 85.

[19] A. Phinyomark, S. Thongpanja, H. Hu, P. Phukpattaranont, C. Limsakul, The usefulness of mean and median frequencies in electromyography analysis, in: G. R. Naik (Ed.), Computational Intelligence in Electromyography Analysis, IntechOpen, Rijeka, 2012, Ch. 8. doi:10.5772/50639.
URL https://doi.org/10.5772/50639

[20] A. Phinyomark, C. Limsakul, P. Phukpattaranont, A novel feature extraction for robust EMG pattern recognition, Journal of Computing 1 (2009) 71–80.

[21] M. Canal, Comparison of wavelet and short time fourier transform methods in the analysis of EMG signals, J Med Syst Feb;34(1):91-4, pMID: 20192059. doi:10.1007/s10916-008-9219-8.

[22] N. Rabin, M. Kahlon, S. Malayev, A. Ratnovsky, Classification of human hand movements based on EMG signals using nonlinear dimensionality reduction and data fusion techniques, Expert Syst. Appl. 149 (2020) 113281.

[23] E. Sejdic, I. Djurovic, J. Jiang, Time–frequency feature representation using energy concentration: An overview of recent advances, Digital Signal Processing 19 (2009) 153–183. doi:10.1016/j.dsp.2007.12.004.

[24] L. Chen, J. Fu, Y. Wu, H. Li, B. Zheng, Hand gesture recognition using compact cnn via surface electromyography signals, Sensors 20 (3). doi:10.3390/s20030672.
URL https://www.mdpi.com/1424-8220/20/3/672

[25] K. Veer, R. Agarwal, Wavelet and short-time fourier transform comparison-based analysis of myoelectric signals, Journal of Applied Statistics 42 (7) (2015) 1591–1601. arXiv:https://doi.org/10.1080/02664763.2014.1001728, doi:10.1080/02664763.2014.1001728.
URL https://doi.org/10.1080/02664763.2014.1001728

[26] A. Moukadem, B. Zied, D. Ould-Abdeslamb, A. Dieterlen, A new optimized Stockwell transform applied on synthetic and real non-stationary signals, Digital Signal Processing (46) (2015) 226–238. doi:10.1016/j.dsp.2015.07.003.
URL https://hal.archives-ouvertes.fr/hal-01291611

[27] Z. Zhu, Tian, Wang, Yokoi, C.-W. Huang, Semg feature extraction based on stockwell transform improves hand movement recognition accuracy, Sensors 19 (2019) 4457. doi:10.3390/s19204457.

[28] I. Jolliffe, Springer-Verlag, Principal Component Analysis, Springer Series in Statistics, Springer, 2002.
URL https://books.google.de/books?id=_olByCrhjwIC

[29] J. . Chu, I. Moon, M. . Mun, A real-time EMG pattern recognition system based on linear-nonlinear feature projection for a multifunction myoelectric hand, IEEE Transactions on Engineering 53 (11) (2006) 2232–2239. doi:10.1109/TBME.2006.883695.

[30] J. J. A. Mendes Junior, M. L. Freitas, H. V. Siqueira, A. E. Lazzaretti, S. F. Pichorim, S. L. Stevan, Feature selection and dimensionality reduction: An extensive comparison in hand gesture classification by sEMG in eight channels armband approach, Signal Processing and Control 59 (2020) 101920. doi:https://doi.org/10.1016/j.bspc.2020.101920.
URL http://www.sciencedirect.com/science/article/pii/S1746809420300768

[31] N. S. Altman, An introduction to kernel and nearest-neighbor nonparametric regression, The American Statistician 46 (3) (1992) 175–185. arXiv:https://www.tandfonline.com/doi/pdf/10.1080/00031305.1992.10475879, doi:10.1080/00031305.1992.10475879.
URL https://www.tandfonline.com/doi/abs/10.1080/00031305.1992.10475879

[32] G. McLachlan, J. W. . Sons, Discriminant Analysis and Statistical Pattern Recognition, Wiley Series in Probability and Statistics, Wiley, 1992.
URL https://books.google.de/books?id=0PFQAAAAMAAJ

[33] C. Cortes, V. Vapnik, Support-vector networks, Machine Learning 20 273–297. doi:10.1023/A:1022627411411.

[34] G. Zhang, Neural networks for classification: a survey, IEEE Transactions on Systems, Man, and Cybernetics, Part C (Applications and Reviews) 30 (4) (2000) 451–462. doi:10.1109/5326.897072.

[35] S. Bhagwat, P. Mukherji, Electromyogram (emg) based fingers movement recognition using sparse filtering of wavelet packet coefficients, Sādhanā 45 (1) (2020) 1–11.

[36] J. Allen, Short term spectral analysis, synthesis, and modification by discrete fourier transform, IEEE Transactions on Acoustics, Speech, and Signal Processing 25 (3) (1977) 235–238. doi:10.1109/TASSP.1977.1162950.

[37] R. G. Stockwell, L. Mansinha, R. P. Lowe, Localization of the complex spectrum: the s transform, IEEE Transactions on Signal Processing 44 (4) (1996) 998–1001. doi:10.1109/78.492555.

[38] M. Jaya Bharata Reddy, R. K. Raghupathy, K. Venkatesh, D. Mohanta, Power quality analysis using discrete orthogonal s-transform (dost), Digital Signal Processing 23 (2) (2013) 616–626. doi:https://doi.org/10.1016/j.dsp.2012.09.013.
URL https://www.sciencedirect.com/science/article/pii/S1051200412002321

[39] R. Stockwell, A basis for efficient representation of the s-transform, Digital Signal Processing 17 (1) (2007) 371 – 393. doi:https://doi.org/10.1016/j.dsp.2006.04.006.
URL http://www.sciencedirect.com/science/article/pii/S1051200406000546

[40] T. Cox, M. Cox, Multidimensional Scaling, Second Edition, 2000. doi:10.1201/9781420036121.

[41] J. Friedman, T. Hastie, R. Tibshirani, et al., The elements of statistical learning, Vol. 1, Springer series in statistics New York, 2001.

[42] F. Azevedo, J. T. Machado, Analysis of electricity markets using multidimensional scaling, in: 2012 9th International Conference on the European Energy Market, 2012, pp. 1–4. doi:10.1109/EEM.2012.6254792.

[43] M. A. Cox, T. F. Cox, Multidimensional scaling, in: Handbook of data visualization, Springer, 2008, pp. 315–347.

[44] J. Tenenbaum, V. Silva, J. Langford, A global geometric framework for nonlinear dimensionality reduction, Science 290 (2000) 2319–2323.

[45] J. Wu, X. Li, W. Liu, Z. Wang, semg signal processing methods: A review, Journal of Physics: Conference Series 1237 (2019) 032008. doi:10.1088/1742-6596/1237/3/032008.

[46] F. F. Chamasemani, Y. P. Singh, Multi-class support vector machine (svm) classifiers – an application in hypothyroid detection and classification, in: 2011 Sixth International Conference on Bio-Inspired Computing: Theories and Applications, 2011, pp. 351–356. doi:10.1109/BIC-TA.2011.51.

[47] M. Asghari Oskoei, H. Hu, Myoelectric control systems—a survey, Signal Processing and Control 2 (4) (2007) 275 – 294. doi:https://doi.org/10.1016/j.bspc.2007.07.009.
URL http://www.sciencedirect.com/science/article/pii/S1746809407000547

[48] D. Tkach, A. Young, L. Smith, E. Rouse, L. Hargrove, Real-time and offline performance of pattern recognition myoelectric control using a generic electrode grid with targeted muscle reinnervation patients, IEEE Trans Neural Syst Rehabil Eng Jul;22(4):727-34, epub 2014 Feb 11. PMID: 24760931. doi:10.1109/TNSRE.2014.2302799.

[49] G. Naik, A. Al-Timemy, H. Nguyen, Transradial amputee gesture classification using an optimal number of sEMG sensors: An approach using ica clustering, IEEE Trans Neural Syst Rehabil Eng Aug;24(8):837-46, epub 2015 Sep 17. PMID: 26394431. doi:10.1109/TNSRE.2015.2478138.

[50] S. Raurale, J. McAllister, J. Martinez del Rincon, Real-time embedded EMG signal analysis for wrist-hand pose identification, IEEE Transactions on Signal Processing 68 (2020) 2713–2723. doi:10.1109/TSP.2020.2985299.

[51] U. Battisti, L. Riba, Window-dependent bases for efficient representations of the stockwell transform, Applied and Computational Harmonic Analysis 40 (2) (2016) 292–320.

[52] K. S. Kim, H. H. Choi, C. S. Moon, C. W. Mun, Comparison of k-nearest neighbor, quadratic discriminant and linear discriminant analysis in classification of electromyogram signals based on the wrist-motion directions, Current applied physics 11 (3) (2011) 740–745.

[53] C. P. Robinson, B. Li, Q. Meng, M. T. Pain, Pattern classification of hand movements using time domain features of electromyography, in: Proceedings of the 4th International Conference on Movement Computing, 2017, pp. 1–6.

[54] G. W. Favieiro, K. O. A. Moura, A. Balbinot, Novel method to characterize upper-limb movements based on paraconsistent logic and myoelectric signals, in: 2016 38th Annual International Conference of the IEEE Engineering in Medicine and Biology Society (EMBC), 2016, pp. 395–398. doi:10.1109/EMBC.2016.7590723.